

AD

RSIC-780

THE THERMOPHYSICAL PROPERTIES OF SOME MULTILAYER INSULATORS AT CYROGENIC TEMPERATURES

by

L. B. Golovanov

Joint Institute for Nuclear Research, Laboratory of High Energy,
Dubna, USSR, pp. 3-20 (1967)

Translated from the Russian

April 1968

This document has been approved for public release and sale;
its distribution is unlimited.

REDSTONE SCIENTIFIC INFORMATION CENTER

REDSTONE ARSENAL, ALABAMA

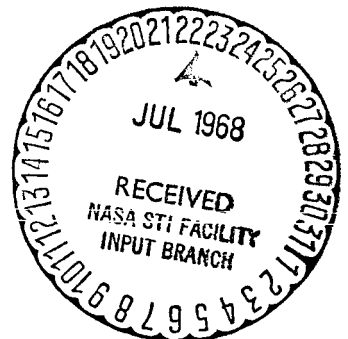
JOINTLY SUPPORTED BY



U.S. ARMY MISSILE COMMAND



GEORGE C. MARSHALL SPACE FLIGHT CENTER



FACILITY FORM 602

N 68-18862
(ACCESSION NUMBER)
23
(PAGES)
TMX-60999
(NASA CR OR TMX OR AD NUMBER)

(THRU)

(CODE)

(CATEGORY)

DISCLAIMER

The findings in this report are not to be construed as an official Department of the Army position unless so designated by other authorized documents.

DISPOSITION

*Destroy this report when it is no longer needed.
Do not return it to the originator.*

10 April 1968

RSIC-780

**THE THERMOPHYSICAL PROPERTIES OF SOME
MULTILAYER INSULATORS AT
CYROGENIC TEMPERATURES**

by

L. B. Golovanov

Joint Institute for Nuclear Research, Laboratory of High Energy,
Dubna, USSR, pp. 3-20(1967)

Translated from the Russian

This document has been approved for public release and sale;
its distribution is unlimited.

Translation Branch
Redstone Scientific Information Center
Research and Development Directorate
U. S. Army Missile Command
Redstone Arsenal, Alabama 35809

THE THERMOPHYSICAL PROPERTIES OF SOME MULTILAYER INSULATORS AT CRYOGENIC TEMPERATURES

by

L. B. Golovanov

The thermal conductivity coefficients for a number of multilayer insulations are given. The dependence of the value of the thermal conductivity coefficient on the pressure in the insulation space, at different compressions of insulation, was found. The coefficient of thermal conductivity was determined at the boundary temperatures 293 to 77.6°K, 293 to 20.4°K, and 294 to 4°K. The insulation was pressed from 1 g/cm² up to 1000 g/cm². The pressure in insulation space varied from 1×10^{-5} to 1×10^{-1} mm Hg.

The Cryogenic Division of the Joint Institute of Nuclear Research had developed a device and the methods of measuring the coefficients of heat conductivity of multilayer insulators.¹ Unlike the existing devices, the new device makes it possible to determine the value of the coefficients of heat conductivity of insulators and also to estimate the error of the measurement. The results obtained by measuring some of the insulators are cited in this article.

The investigation disclosed a relationship between the coefficient of heat conductivity of insulators, the pressure in the insulated space, and the specific pressure applied to the insulators. The investigation was carried out at constant boundary of warm temperature (293°K) and at various boundary cold temperatures: nitric, hydrogen, and helium. Also found was the relationship between the specific pressure on insulators and the relative deformation, number of layer per 1 cm of thickness, and the weight by volume of multilayer insulators.

SELECTING THE RANGE OF CHANGES IN PARAMETERS WHICH AFFECT THE VALUE OF THE COEFFICIENT OF HEAT CONDUCTIVITY OF INSULATORS

The Pressure in the Insulated Space

The pressure in the insulated space varied from 1×10^{-5} to 1×10^{-1} mm Hg. The choice of the lower pressure limit of 1×10^{-5} mm Hg was based

¹L. B. Golovanov, OSOBENNOSTI IZMERENIYA KOEFFITSIENTOV TEPLOPROVODNOSTI MNOGOSLOYNYKH IZOLYATSIY (Special Features in Measuring the Coefficients of Heat Conductivity of Multilayer Insulations), preprint R8-3236 of OIYaI (Joint Institute of Nuclear Research), Dubna, 1967.

on the fact that such a vacuum can be produced by a conventional diffusion pump - also, because beginning with a pressure of 1×10^{-4} and below, the coefficient of heat conductivity ρ of multilayer insulators depends on the pressure. The choice of upper limit of 1×10^{-1} mm Hg of pressure was influenced by the ease with which this pressure can be obtained with the aid of an ordinary forevacuum pump. The coefficient of heat conductivity of the insulators was measured at 20.4°K as the cold-wall temperature at pressures varying from 1×10^{-5} to 1×10^{-2} mm Hg, while at a cold-wall temperature of 4.2°K, the pressure varied between 1×10^{-5} and 1×10^{-3} mm Hg. Reduced pressure ranges were used because the use of multilayer insulations at the initial vacuum for heat insulating of liquid hydrogen and helium is expedient due to the low heat of evaporation of these liquids and to the comparatively large coefficient of insulator's heat conductivity at the initial vacuum.

The Specific Pressure on the Insulation

The specific pressure on the insulation varied from 1 to 1000 g/cm². The choice of the lower limit of 1 g/cm² was governed by the following considerations:

1. Under actual conditions it is extremely difficult to insulate surfaces (particularly horizontal surfaces) by compressing the insulation with a pressure of less than 1 g/cm².
2. A specific pressure of 1 g/cm² is only several times larger than pressure exerted by the weight of the specimen.
3. In determining the coefficient of heat conductivity of an insulation under a load close to zero, there will appear errors due to the indeterminacy of the contact between the insulation layers and the cold surface of the device because a part of the heat flux from the face of the insulation is not removed by the surface of the protective tank.

The choice of the upper limit of 1000 g/cm² was determined by the design of the vessels in which both or one of the walls (inside or outside) were flexible.

The Accuracy of the Measurements

The accuracy in measuring the coefficient of heat conductivity with the method of OIYaI (Joint Institute for Nuclear Research) varied on the average from 18 to 40 percent. The pressure in the insulating space was measured with an accuracy not exceeding 20 percent. The specific pressure on the insulation was determined with an accuracy of 10 percent.

The Properties of the Insulators

Let us first consider the mechanical properties of the insulation, such as the relationship between the specific pressure applied to the insulation and the volumetric weight, number of layers per 1 cm of thickness, and the coefficient of relative deformation. The investigated insulation specimens which had as their gasket materials SBR-sandpaper 50 μ thick and EVTI spun glass 100 μ thick were shielded by aluminum-plated lavsan-films 12 μ thick and aluminum foil with 10 and 30 μ in thickness.

The relationship between the volumetric weight of the listed insulations and the specific pressure applied to them is shown in Figure 1.

Figure 1 shows that, depending on the thickness and density of the material, the volumetric weight of the insulation varies from 100 to 200 kg/m^3 when the load on the insulation is 1 g/cm^2 and from 300 to 600 kg/m^3 for a load equal to 1000 g/cm^2 . On the average, there is a threefold increase in the volumetric weight of the insulation compressed from 1 to 1000 g/cm^2 .

Figure 2 shows the relationship between the number of layers per 1 cm of thickness and the specific pressure applied to the insulation. The number of layers for an insulation with a gasket material made of spun glass is about 20 layers per centimeter for a specific pressure of 1 g/cm^2 ; it is equal to 30 layers per centimeter for sandpaper. As the load is increased to 1000 g/cm^2 , the number of layers increases to 60 layers per centimeter for spun glass and to 150 layers per centimeter for sandpaper.

The relationship between the coefficient of relative deformation and the specific pressure on the insulation is shown in Figure 3. The coefficient of the relative deformation was defined as the ratio of the height of a specimen under a load p to the height of the an insulation specimen under a load of 1 g/cm^2 . Under a load of 1000 g/cm^2 , the coefficient of relative deformation varies from 0.31 to 0.37, depending on the properties of the gasket material and of the shields.

Let us consider the affect of various factors on the value of the coefficient of heat conductivity.

In Figure 4 is shown the relationship between the coefficient of heat conductivity of a multilayer insulation consisting of sandpaper and aluminum plated lavsan-film and the pressure in the insulating space at different forces compressing the insulation. In determining the values of the coefficient of heat conductivity there were also found errors in the measurements; for example, the coefficient of heat conductivity of a given insulator with 1×10^{-5} mm Hg as

the pressure in the insulating space and 1 g/cm^2 as the specific pressure on the insulation is equal to $\lambda = \begin{pmatrix} +0.2 \\ 1.1 -0.1 \end{pmatrix} 10^{-4} \text{ mm Hg}$, while for a pressure of $1 \times 10^{-1} \text{ mm Hg}$ it is $\lambda = \begin{pmatrix} +4.1 \\ 19 -2.7 \end{pmatrix} 10^{-4} \text{ W/m degree}$. The curves show that the coefficient of heat conductivity of insulation compressed by a force of 1 g/cm^2 is independent of the pressure in the insulating space beginning with $1 \times 10^{-4} \text{ mm Hg}$ and below; for insulation compressed with a force of 1000 g/cm^2 , the coefficient of heat conductivity is independent of the pressure beginning with $1 \times 10^{-3} \text{ mm Hg}$ and lower. With the insulation compressed from 1 to 1000 g/cm^2 and a pressure in the insulating space equal to $1 \times 10^{-5} \text{ mm Hg}$, the coefficient of heat conductivity increases approximately six times. In case of a declining vacuum, the coefficients of heat conductivity of insulation at 1 and 1000 g/cm^2 are increasing and come close to one another. At a pressure of $6 \times 10^{-2} \text{ mm Hg}$ they become equal.

Figure 5 shows the relationship between the heat conductivity of the same insulation used in Figure 4 and the specific pressure applied to it at various pressures in the insulating space. It is well shown there that, at a pressure of less than $1 \times 10^{-2} \text{ mm Hg}$ in the insulating space, the coefficient of heat conductivity increases monotonically with the increase in the load on the insulation. At a pressure larger than $1 \times 10^{-2} \text{ mm Hg}$, an increased load on the insulation causes the coefficient of conductivity to decrease at the beginning and, upon reaching a minimum at a specific pressure of about 100 g/cm^2 , the coefficient begins to increase.

In the lower part of Figure 5 is drawn a broken-line horizontal whose ordinate is equal to the value of the coefficient of heat conductivity of the given insulation measured at a vacuum of $1 \times 10^{-5} \text{ mm Hg}$ without a load on the insulation, i. e., a minimum coefficient of heat conductivity $\lambda_{\min} = 0.6 \times 10^4$ mm Hg. Knowing the value of the minimum coefficient of heat conductivity, it is possible to estimate the share of three types of heat transfer existing in multilayer insulation, namely: the heat transfer by radiation, by contacts, and by residual gases in the common thermal flux through the insulation at various pressures in the insulating space and specific loads applied to it. For example, the overall thermal flux through the insulation with $4 \times 10^{-3} \text{ mm Hg}$ as the pressure in the insulating space and 3 g/cm^2 as the pressure applied to the insulation will be proportional to section a-d. The thermal flux by radiation will be proportional to the section a-b included between the axis of the abscissae and the horizontal line corresponding to the minimum coefficient of heat conductivity of the insulation. The thermal flux through the contacts is proportional to the section b-c confined between the horizontal line corresponding to λ_{\min}

and the curve corresponding to the coefficient of the insulation's heat conductivity at a pressure of 1×10^{-5} mm Hg. The thermal flux by the residual gases is determined by the section c-d confined between the curves corresponding to coefficients of heat conductivity at pressure in the insulating space equal to 1×10^{-5} and 4×10^{-3} mm Hg. The division of the overall thermal flux into its components is just for orientation, because in reality all types of heat transfer are mutually related.

Figures 6 and 7 show the coefficients of heat conductivity of insulation consisting of spun glass and aluminum-plated lavsan-film as functions of the pressure in the insulating space and the specific pressure applied to the insulation. As shown, the character of the curves is the same as in Figures 4 and 5 and the only difference is in the absolute values of the coefficients of heat conductivity. The minimum value of the insulation's coefficient of heat conductivity at a vacuum of 1×10^{-5} mm Hg without pressure on the insulation is $\lambda_{\min} = 0.9 \times 10^{-4}$ W/m degree. This value corresponds to the broken straight line in Figure 7. At a specific pressure of 1 g/cm^2 and a vacuum of 1×10^{-5} mm Hg, the coefficient of heat conductivity of the insulation is $\lambda = 1.7 \times 10^{-4}$ W/m degree. The coefficient of heat conductivity is considerably larger at a pressure of 1×10^{-1} mm Hg and at a specific pressure on the insulation of 1 g/cm^2 . It is equal to $\lambda = \begin{pmatrix} +5.7 \\ 29.3 - 3.7 \end{pmatrix} \times 10^{-4}$ W/m degree. Therefore, it shows that an insulation with a number of shields nearly twice as many per unit of length has a coefficient of conductivity which is two times smaller.

The effect of the material of the shields of a multilayer insulation on the coefficient of heat conductivity is shown in Figure 8. A comparison is made in Figure 8a of two specimens of insulation with sandpaper as the gasket material. The shield in one specimen are made of aluminized lavsan (the lighter points on the curves), and the shield of the other specimen is made of aluminum foil (dark points on the curves). By comparing these specimens it can be concluded that the coefficient of heat conductivity of insulation with lavsan shields is somewhat smaller than that of an insulation with aluminum foil shields only when the insulation is compressed with a force of 1 g/cm^2 ; however, an opposite picture is obtained for a compression of approximately 1000 g/cm^2 , where the coefficient of heat conductivity of an insulation with an aluminum foil shield is lower than that of an insulation with shields made of aluminized lavsan. Similar results shown in Figure 8b were obtained by investigating multilayer insulations using the other gasket material (spun glass).

In Figures 9 and 10 are given the results obtained by measuring the coefficient of heat conductivity of an insulation consisting of sandpaper and an

aluminized lavsan-film at the boundary temperatures 293 and 4.2°K (Figures 8a and 10a) and 293 and 20.4°K (Figures 9b and 10b). For comparing the coefficients of heat conductivity obtained at different temperatures of the cold wall, Figure 11 shows the ratios of the coefficients of heat conductivity of an insulation consisting of sandpaper and aluminized lavsan-film measured at the boundary temperatures of 293 and 77.8°K and at 293 and 20.4°K as a function of the pressure in the insulating space and of the specific pressure on the insulation. The same relationships as in Figure 11 are also given in Figure 12, but for the ratios of coefficients of heat conductivity measured with the cold wall at the boundary helium and nitric temperatures.

Figure 11 shows that the coefficient of heat conductivity of the same insulation measured at the temperature of liquid hydrogen is 0.88 to 0.6, or is on the average 0.74 times smaller than the coefficient of heat conductivity measured at the temperature of liquid nitrogen, while the ratio of the boundary temperatures: $(293-20)/(293-77)$ is equal to 0.79 (shown by broken line in Figure 11). A similar picture is observed also in measurements with helium. Figure 12 shows that the insulation's coefficient of heat conductivity measured at the temperature of liquid helium is 0.8 - 0.65, or on the average is 0.72 times smaller than the coefficient of heat conductivity measured at the temperature of liquid nitrogen, and the ratio of the boundary temperatures is equal to 0.745 (shown by broken line in Figure 12). This makes it possible to conclude that the value of the thermal flux through the insulation does not depend on the boundary cold temperature when the temperature-range amounts to 77.8 - 4.2°K.

The author is grateful to N. I. Balandikov, V. L. Nekhayevskiy, Ye. A. Kozyreva, A. A. Goryunov, A. P. Tsvinev, A. I. Kalmykova, V. I. Kostirko, and to V. P. Vlasov for the assistance in carrying out the experiments and in processing the results.

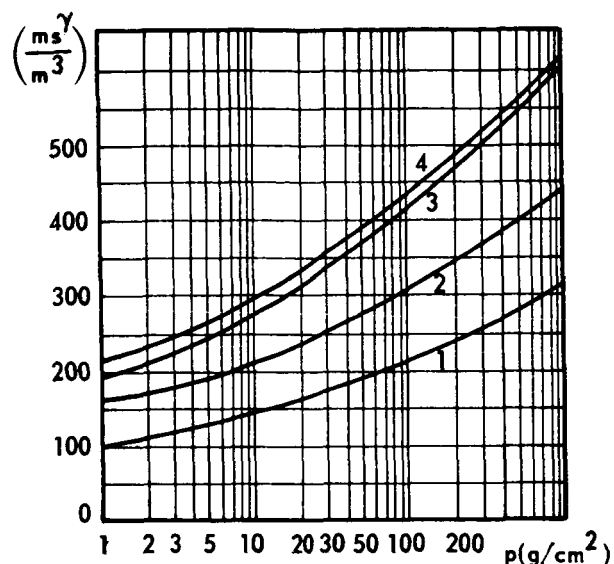


Figure 1. The relationship between the volumetric weight γ of the insulation and the pressure p applied to the insulation. 1) EVTI-spun glass 100 mm thick and aluminized lavsan-film 12 μ in thickness; 2) SBR-sandpaper 50 μ thick and aluminized lavsan-film 12 μ thick; 3) SBR-sandpaper 50 μ thick and aluminum foil 10 μ in thickness; 4) EVTI-spun glass 100 μ thick and aluminum foil 30 μ in thickness.

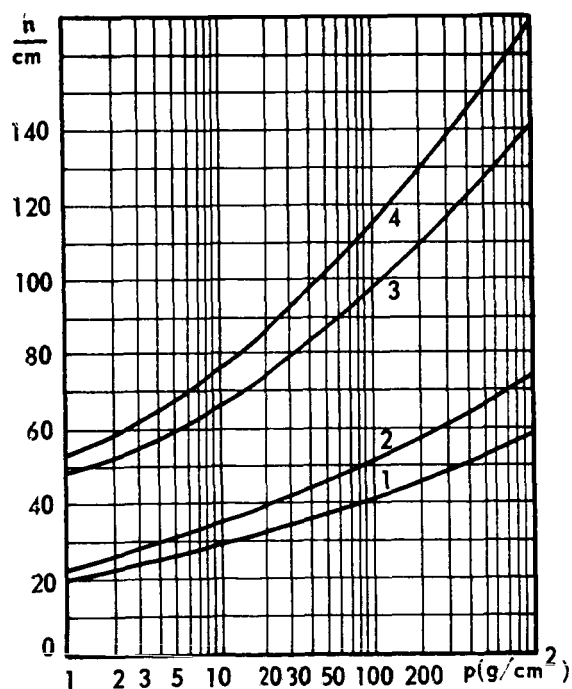


Figure 2. The relationship between the number of layers n per 1 cm of thickness of insulation and the specific pressure p applied to the insulation. 1) EVTI-spun glass 100 μ thick and aluminized lavsan-film 12 μ thick; 2) SBR-sandpaper 59 μ thick and aluminized lavsan-film 12 μ thick; 3) SBR-sandpaper 50 μ thick and aluminum foil 10 μ in thickness.

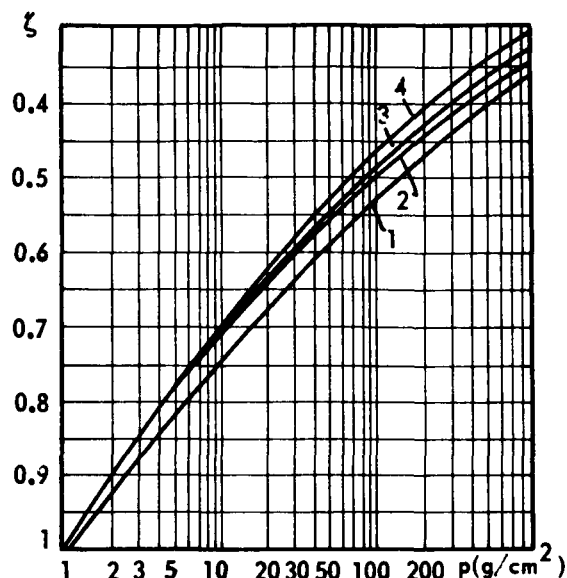


Figure 3. The coefficient of relative deformation ζ as a function of the specific pressure p applied to the insulation. 1) SBR-sandpaper 50 μ thick and aluminized lavsan-film 12 μ thick; 2) EVTI-spun glass 100 μ thick and aluminum foil 50 μ in thickness; 3) SBR-sandpaper 50 μ thick and aluminum foil 10 μ in thickness; 4) EVTI-spun glass 100 μ thick and aluminized lavsan-film 12 μ in thickness.

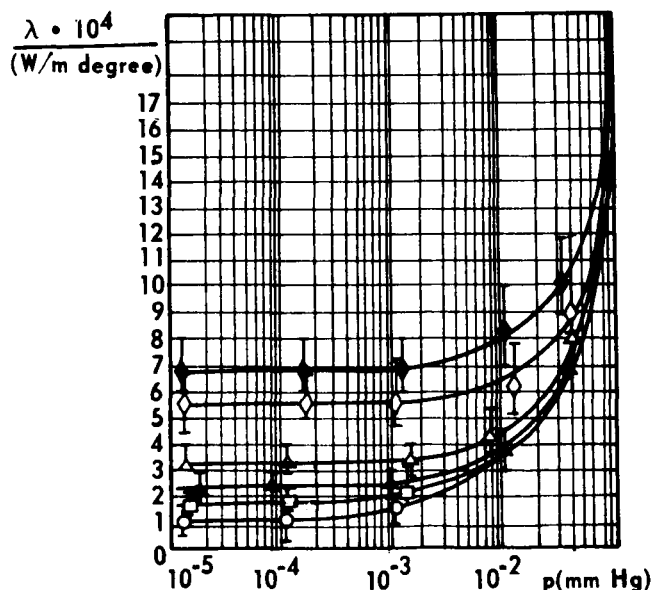


Figure 4. The relationship between the coefficient of heat conductivity λ of an insulation consisting of 50 μ thick SBR-sandpaper and 12 μ thick aluminized lavsan-film and the pressure p in the insulating space (the boundary temperatures are 293 and 77.8°K, the residual gas is nitrogen) at a specific pressure on the insulation, in g/cm^2 , \circ -1, \square -8, \triangle -35, \blacktriangle -120, \diamond -550, \blacklozenge -800.

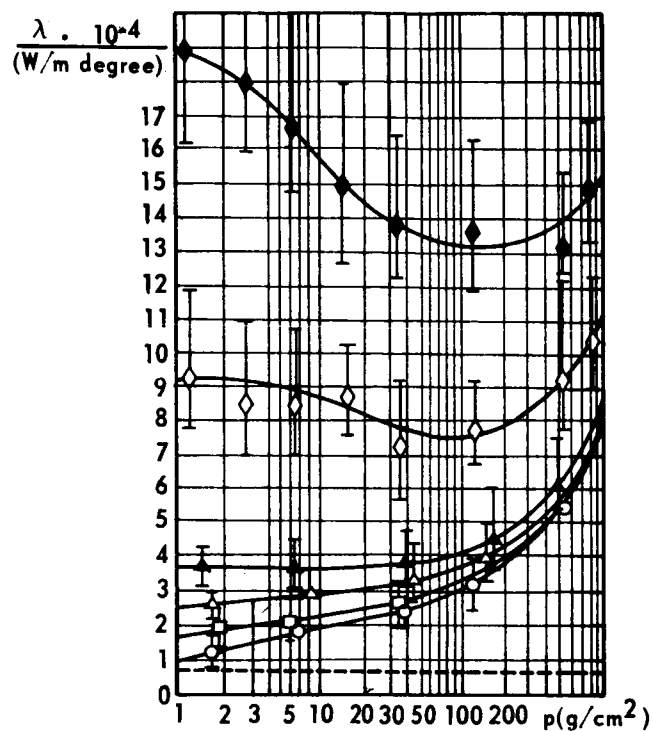


Figure 5. The coefficient of heat conductivity λ of an insulation consisting of 50 μ thick SBR-sandpaper and 12 μ thick aluminized lavsan-film as a function of the specific pressure p on the insulation (293 and 77°K as boundary temperatures and nitrogen as the residual gas) at pressures in insulating space, in mm Hg, \circ - 1×10^{-5} , \square - 1×10^{-3} , \triangle - 4×10^{-3} , \blacklozenge - 1×10^{-2} , \diamond - 4×10^{-2} , \blacklozenge - 10^{-1}

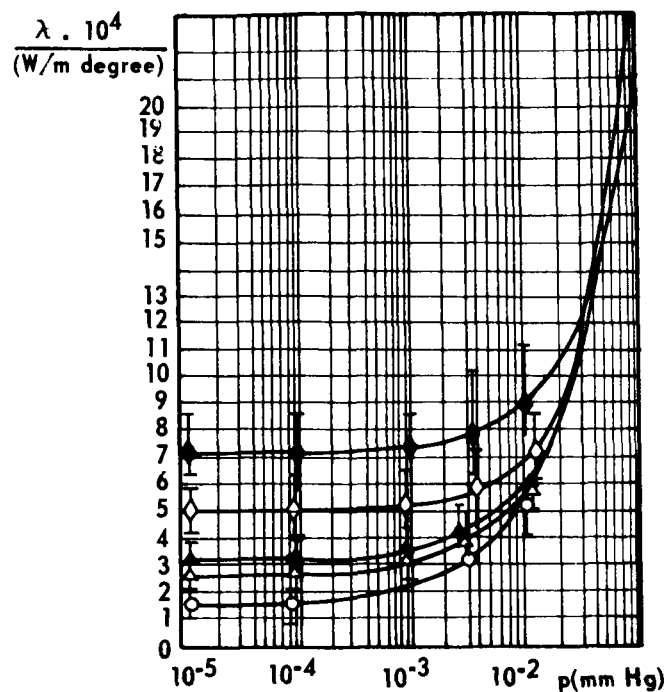


Figure 6. The coefficient of heat conductivity λ of insulation consisting of 100μ thick EVTI-spun glass and aluminized 12μ thick lavsan-film as a function of the pressure in the insulating space P (the boundary temperatures are 293 and 77.8°K and the residual gas is nitrogen) at pressures on the insulation p , in g/cm^2 , \circ - 1, \triangle - 25, \blacktriangle - 70, \diamond - 270, \blacklozenge - 700.

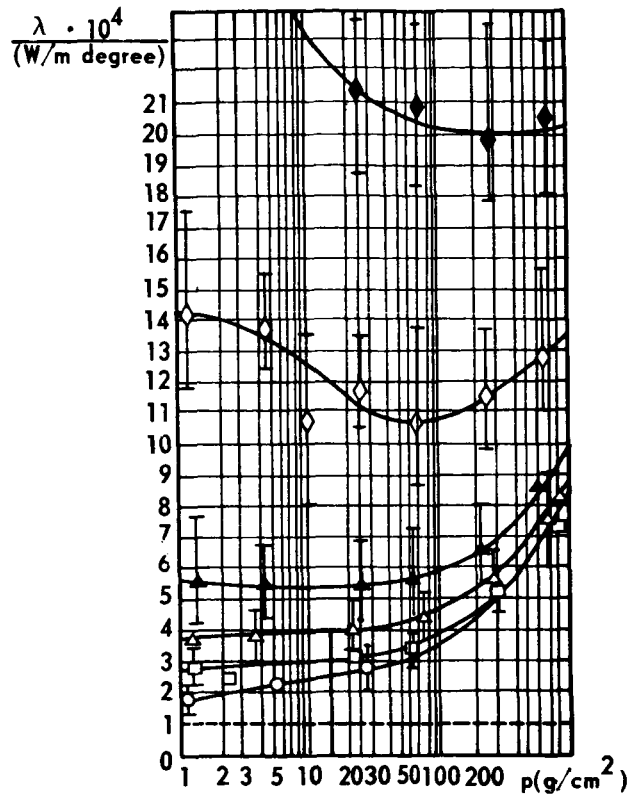


Figure 7. The coefficient of heat conductivity λ of an insulator consisting of 100μ thick EVTI spun glass and 12μ thick aluminized lavsan-film as a function of the specific pressure p on the insulation (293 and 77.8°K are the boundary temperatures and nitrogen is the residual gas) at pressures in the insulating space P , in mm Hg, $\circ - 1 \times 10^{-5}$, $\blacksquare - 1 \times 10^{-3}$, $\blacktriangle - 4 \times 10^{-3}$, $\triangle - 1 \times 10^{-2}$, $\diamond - 4 \times 10^{-2}$, $\blacklozenge - 1 \times 10^{-1}$.

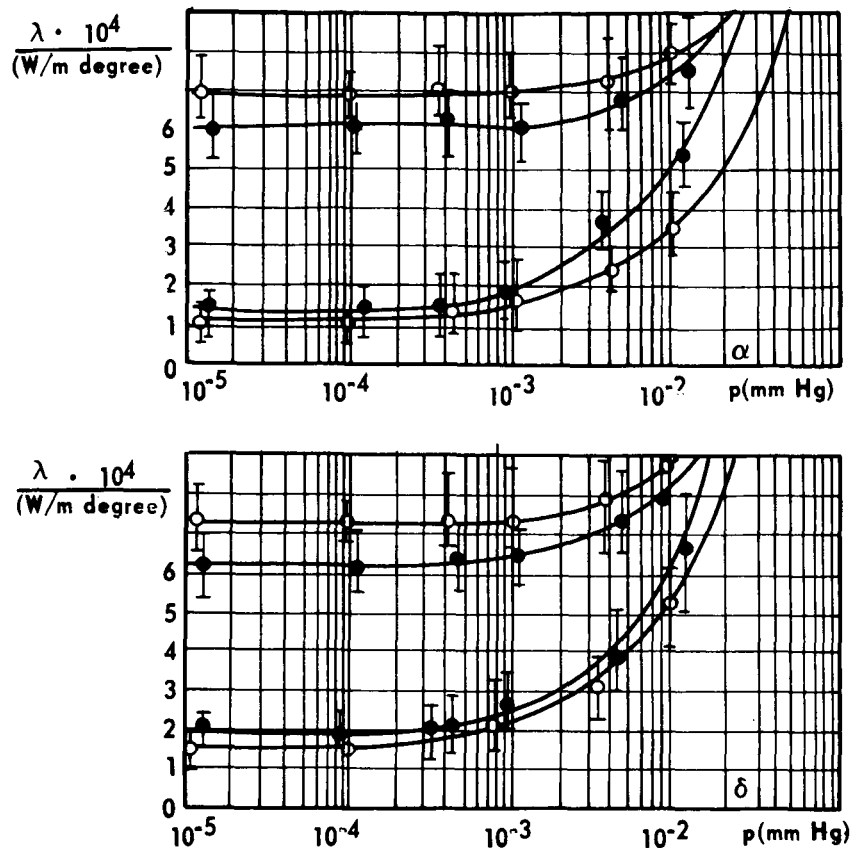


Figure 8. The relationship between the coefficient of heat conductivity λ and the pressure in the insulating space for specimen consisting of: a) 50μ thick SBR-sandpaper and \circ 12μ thick aluminized lavsan-film and \bullet 10μ thick aluminum foil; b) 100μ thick EVTI spun glass, \circ 12μ thick aluminized lavsan-film; \bullet 30μ thick aluminum foil.

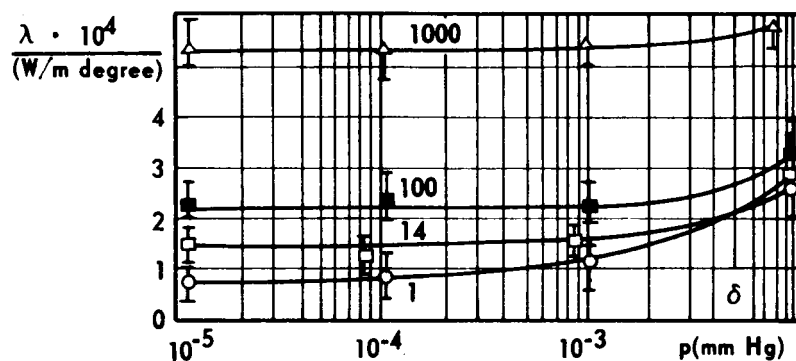
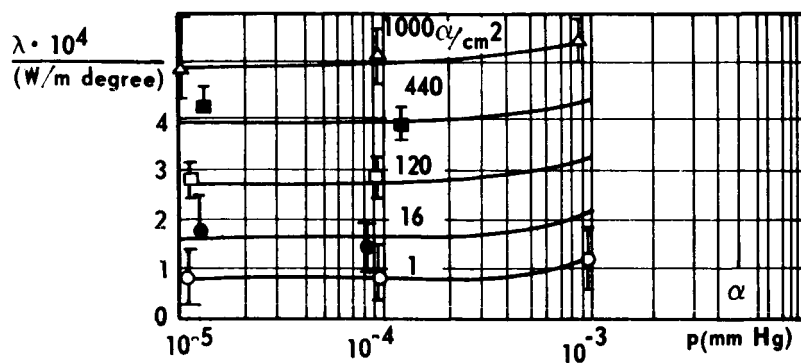


Figure 9. The coefficient of heat conductivity λ of insulator consisting of 50μ thick SBR-sandpaper and 12μ thick aluminized lavesan-film as a function of the specific pressure on the insulation at various pressures in the insulating space P , in mm Hg, (a - boundary temperatures are 293 and 4.2°K , the residual gas is helium; b - boundary temperatures are 293 and 20.4°K with hydrogen as the residual gas).

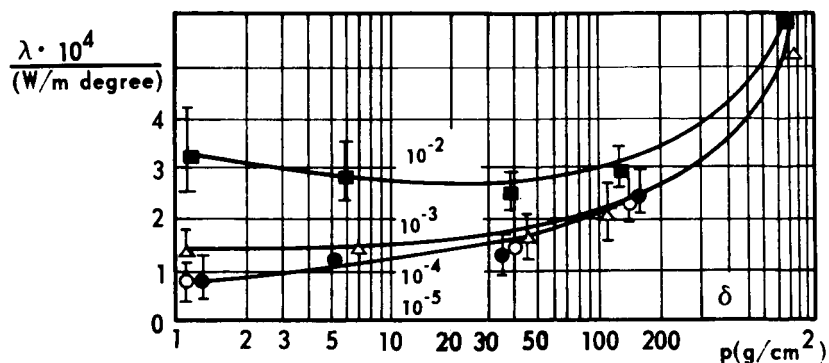
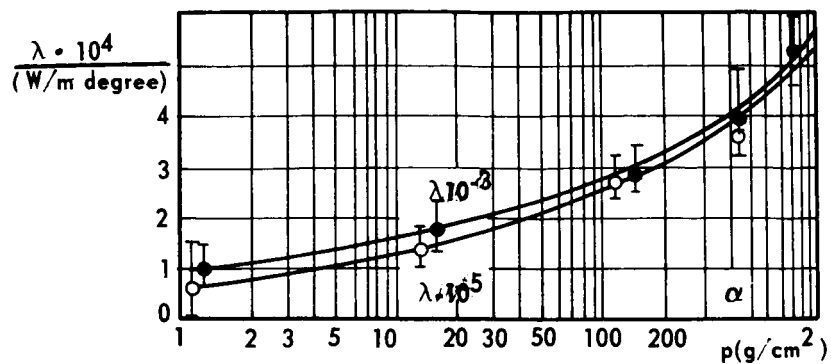


Figure 10. Coefficient of heat conductivity λ of insulator consisting of 50μ thick SBR-sandpaper and 12μ thick aluminized lavsan-film as a function of the specific pressure on the insulation, at various pressures in the insulating space P , in mm Hg (a - 293 and 4.2°K as boundary temperatures and helium as residual gas; b - 293 and 20.4°K as boundary temperatures and hydrogen as residual gas).

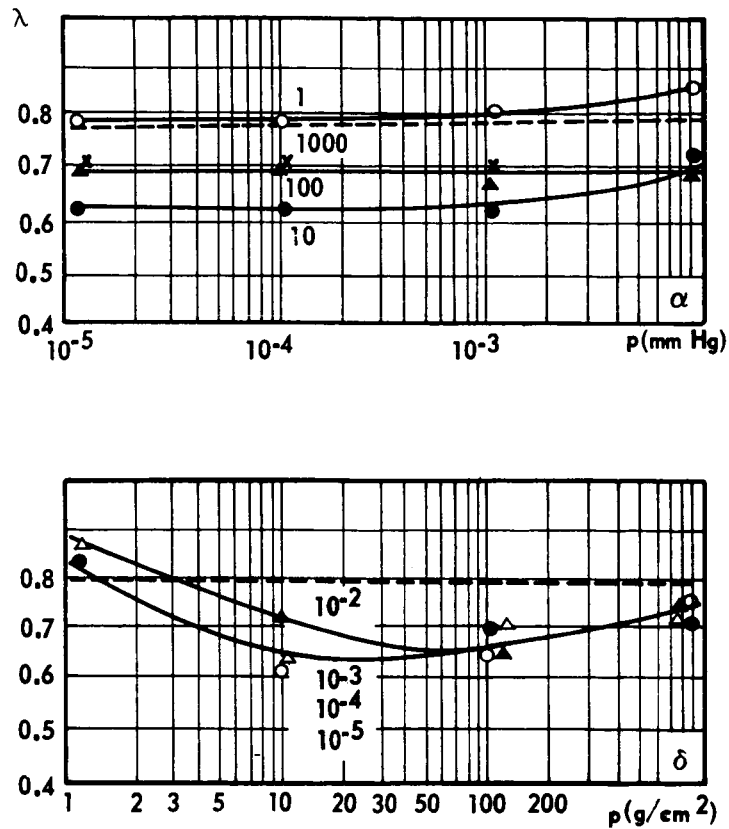


Figure 11. Relationship between the ratios of coefficients of heat conductivity λ of insulation consisting of 50μ thick SBR-sandpaper and 12μ thick aluminized lavsan-film measured at boundary temperatures of 293 and 77.8°K and at 293 and 20.4°K and: a) the pressure in the insulating space at various specific pressures on the insulation p , in g/cm²; b) and the specific pressure P on the insulation at various pressures in the insulating space p , in mm Hg.

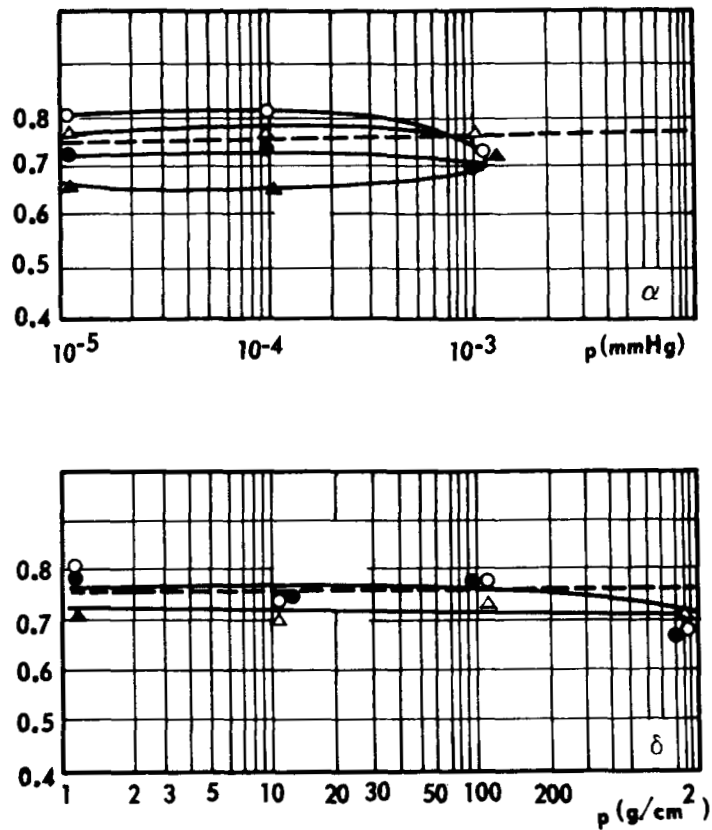


Figure 12. The ratios of coefficients of heat conductivity of insulator consisting of 50μ thick SBR-sandpaper and 12μ thick aluminized lavsan-film measured at boundary temperatures of 293 and 77.8°K and at 293 and 4.2°K as functions of: a) of the pressure in the insulating space at various pressures p on the insulation, in g/cm^2 ; b) of the specific pressure on the insulation at various pressures in the insulating space P , in mm Hg.

DISTRIBUTION

	No. of Copies		No. of Copies
<u>EXTERNAL</u>		U. S. Atomic Energy Commission	1
Air University Library	1	ATTN: Reports Library, Room G-017	
ATTN: AUL3T		Washington, D. C. 20545	
Maxwell Air Force Base, Alabama 36112		U. S. Naval Research Laboratory	1
U. S. Army Electronics Proving Ground	1	ATTN: Code 2027	
ATTN: Technical Library		Washington, D. C. 20390	
Fort Huachuca, Arizona 85613		Weapons Systems Evaluation Group	1
Naval Weapons Center	1	Washington, D. C. 20305	
ATTN: Technical Library, Code 753		John F. Kennedy Space Center, NASA	2
China Lake, California 93555		ATTN: KSC Library, Documents Section	
Naval Weapons Center, Corona Labs.	1	Kennedy Space Center, Florida 32899	
ATTN: Documents Librarian		APGC (PGBPS-12)	1
Corona, California 91720		Eglin Air Force Base, Florida 32542	
Lawrence Radiation Laboratory	1	U. S. Army CDC Infantry Agency	1
ATTN: Technical Information Division		Fort Benning, Georgia 31905	
P. O. Box 808		Argonne National Laboratory	1
Livermore, California 94550		ATTN: Report Section	
Sandia Corporation	1	9700 South Cass Avenue	
ATTN: Technical Library		Argonne, Illinois 60440	
P. O. Box 969		U. S. Army Weapons Command	1
Livermore, California 94551		ATTN: AMSWE-RDR	
U. S. Naval Postgraduate School	1	Rock Island, Illinois 61201	
ATTN: Library		Rock Island Arsenal	1
Monterey, California 93940		ATTN: SWERI-RDI	
Electronic Warfare Laboratory, USAECOM	1	Rock Island, Illinois 61201	
Post Office Box 205		U. S. Army Cmd. & General Staff College	1
Mountain View, California 94042		ATTN: Acquisitions, Library Division	
Jet Propulsion Laboratory	2	Fort Leavenworth, Kansas 66027	
ATTN: Library (TDS)		Combined Arms Group, USACDC	1
4800 Oak Grove Drive		ATTN: Op. Res., P and P Div.	
Pasadena, California 91103		Fort Leavenworth, Kansas 66027	
U. S. Naval Missile Center	1	U. S. Army CDC Armor Agency	1
ATTN: Technical Library, Code N3022		Fort Knox, Kentucky 40121	
Point Mugu, California 93041		Michoud Assembly Facility, NASA	1
U. S. Army Air Defense Command	1	ATTN: Library, I-MICH-OSD	
ATTN: ADSX		P. O. Box 29300	
Ent Air Force Base, Colorado 80912		New Orleans, Louisiana 70129	
Central Intelligence Agency	4	Aberdeen Proving Ground	1
ATTN: OCR/DD-Standard Distribution		ATTN: Technical Library, Bldg. 313	
Washington, D. C. 20505		Aberdeen Proving Ground, Maryland 21005	
Harry Diamond Laboratories	1	NASA Sci. & Tech. Information Facility	5
ATTN: Library		ATTN: Acquisitions Branch (S-AK/DL)	
Washington, D. C. 20438		P. O. Box 33	
Scientific & Tech. Information Div., NASA	1	College Park, Maryland 20740	
ATTN: ATS		U. S. Army Edgewood Arsenal	1
Washington, D. C. 20546		ATTN: Librarian, Tech. Info. Div.	
		Edgewood Arsenal, Maryland 21010	

	No. of Copies		No. of Copies
National Security Agency ATTN: C3/TDL Fort Meade, Maryland 20755	1	Brookhaven National Laboratory Technical Information Division ATTN: Classified Documents Group Upton, Long Island, New York 11973	1
Goddard Space Flight Center, NASA ATTN: Library, Documents Section Greenbelt, Maryland 20771	1	Watervliet Arsenal ATTN: SWEV-RD Watervliet, New York 12189	1
U. S. Naval Propellant Plant ATTN: Technical Library Indian Head, Maryland 20640	1	U. S. Army Research Office (ARO-D) ATTN: CRD-AA-IP Box CM, Duke Station Durham, North Carolina 27706	1
U. S. Naval Ordnance Laboratory ATTN: Librarian, Eva Liberman Silver Spring, Maryland 20910	1	Lewis Research Center, NASA ATTN: Library 21000 Brookpark Road Cleveland, Ohio 44135	1
Air Force Cambridge Research Labs. L. G. Hanscom Field ATTN: CRMCLR/Stop 29 Bedford, Massachusetts 01730	1	Foreign Technology Division ATTN: Library Wright-Patterson Air Force Base, Ohio 45400	1
U. S. Army Tank Automotive Center ATTN: SMOTA-RTS.1 Warren, Michigan 48090	1	U. S. Army Artillery & Missile School ATTN: Guided Missile Department Fort Sill, Oklahoma 73503	1
U. S. Army Materials Research Agency ATTN: AMXMR-ATL Watertown, Massachusetts 02172	1	U. S. Army CDC Artillery Agency ATTN: Library Fort Sill, Oklahoma 73504	1
Strategic Air Command (OAI) Offutt Air Force Base, Nebraska 68113	1	U. S. Army War College ATTN: Library Carlisle Barracks, Pennsylvania 17013	1
Picatinny Arsenal, USAMUCOM ATTN: SMUPA-VA6 Dover, New Jersey 07801	1	U. S. Naval Air Development Center ATTN: Technical Library Johnsville, Warminster, Pennsylvania 18974	1
U. S. Army Electronics Command ATTN: AMSEL-CB Fort Monmouth, New Jersey 07703	1	Frankford Arsenal ATTN: C-2500-Library Philadelphia, Pennsylvania 19137	1
Sandia Corporation ATTN: Technical Library P. O. Box 5800 Albuquerque, New Mexico 87115	1	Div. of Technical Information Ext., USAEC P. O. Box 62 Oak Ridge, Tennessee 37830	1
ORA(RRRT) Holloman Air Force Base, New Mexico 88330	1	Oak Ridge National Laboratory ATTN: Central Files P. O. Box X Oak Ridge, Tennessee 37830	1
Los Alamos Scientific Laboratory ATTN: Report Library P. O. Box 1663 Los Alamos, New Mexico 87544	1	Air Defense Agency, USACDC ATTN: Library Fort Bliss, Texas 79916	1
White Sands Missile Range ATTN: Technical Library White Sands, New Mexico 88002	1	U. S. Army Air Defense School ATTN: AKBAAS-DR-R Fort Bliss, Texas 79906	1
Rome Air Development Center (EMLAL-1) ATTN: Documents Library Griffiss Air Force Base, New York 13440	1		

	No. of Copies		No. of Copies
U. S. Army Combat Developments Command Institute of Nuclear Studies Fort Bliss, Texas 79916	1	<u>INTERNAL</u>	
Manned Spacecraft Center, NASA ATTN: Technical Library, Code BM6 Houston, Texas 77058	1	Headquarters U. S. Army Missile Command Redstone Arsenal, Alabama 35809	
Defense Documentation Center Cameron Station Alexandria, Virginia 22314	20	ATTN: AMSMI-D	1
U. S. Army Research Office ATTN: STINFO Division 3045 Columbia Pike Arlington, Virginia 22204	1	AMSMI-XE, Mr. Lowers	1
		AMSMI-Y	1
		AMSMI-R, Mr. McDaniel	1
		AMSMI-RAP	1
		AMSMI-RBLD	10
		USACDC-LnO	1
		AMSMI-RBT	8
		AMSMI-RB, Mr. Croxton	1
U. S. Naval Weapons Laboratory ATTN: Technical Library Dahlgren, Virginia 22448	1	National Aeronautics & Space Administration Marshall Space Flight Center ATTN: MS-T, Mr. Wiggins	5
U. S. Army Engineer Res. & Dev. Labs. ATTN: Scientific & Technical Info. Br. Fort Belvoir, Virginia 22060	2	Marshall Space Flight Center, Ala. 35812	
Langley Research Center, NASA ATTN: Library, MS-185 Hampton, Virginia 23365	1		
Research Analysis Corporation ATTN: Library McLean, Virginia 22101	1		
Foreign Science & Technology Center Munitions Building Washington, D. C. 20315	3		
National Aeronautics & Space Administration Code USS-T (Translation Section) Washington, D. C. 20546	2		

UNCLASSIFIED

Security Classification

DOCUMENT CONTROL DATA - R & D

(Security classification of title, body of abstract and indexing annotation must be entered when the overall report is classified)

1. ORIGINATING ACTIVITY (Corporate author) Redstone Scientific Information Center Research and Development Directorate U. S. Army Missile Command Redstone Arsenal, Alabama 35809		2a. REPORT SECURITY CLASSIFICATION Unclassified	
		2b. GROUP N/A	
3. REPORT TITLE THE THERMOPHYSICAL PROPERTIES OF SOME MULTILAYER INSULATORS AT CRYOGENIC TEMPERATURES Joint Institute for Nuclear Research, Laboratory of High Energy, Dubna, USSR, pp. 3-20 (1967)			
4. DESCRIPTIVE NOTES (Type of report and inclusive dates) Translated from the Russian			
5. AUTHOR(S) (First name, middle initial, last name) L. B. Golovanov			
6. REPORT DATE 10 April 1968		7a. TOTAL NO. OF PAGES 19	7b. NO. OF REFS 0
8a. CONTRACT OR GRANT NO. N/A		9a. ORIGINATOR'S REPORT NUMBER(S) RSIC-780	
b. PROJECT NO. N/A		9b. OTHER REPORT NO(S) (Any other numbers that may be assigned this report)	
c.		AD _____	
d.			
10. DISTRIBUTION STATEMENT This document has been approved for public release and sale; its distribution is unlimited.			
11. SUPPLEMENTARY NOTES None		12. SPONSORING MILITARY ACTIVITY Same as No. 1	
13. ABSTRACT The thermal conductivity coefficients for a number of multilayer insulations are given. The dependence of the value of the thermal conductivity coefficient on the pressure in the insulation space, at different compressions of insulation, was found. The coefficient of thermal conductivity was determined at the boundary temperatures 293 to 77.6°K, 293 to 20.4°K, and 293 to 4°K. The insulation was pressed from 1 g/cm ² up to 1000 g/cm ² . The pressure in insulation space varied from 1 × 10 ⁻⁵ to 1 × 10 ⁻¹ mm Hg.			

DD FORM 1473

REPLACES DD FORM 1473, 1 JAN 64, WHICH IS OBSOLETE FOR ARMY USE.

UNCLASSIFIED

Security Classification

21

UNCLASSIFIED

Security Classification

14.	KEY WORDS	LINK A		LINK B		LINK C	
		ROLE	WT	ROLE	WT	ROLE	WT
	Thermal conductivity coefficients Multilayer insulators Specific pressure Boundary temperatures Thermal flux						

UNCLASSIFIED

Security Classification